# Desaturation Controller for a Magnetic Core

Jinhua Wang<sup>1</sup>, Jaehoon Kim<sup>2</sup>, and Dong Sam Ha<sup>1</sup>

<sup>1</sup>Multifunctional Integrated Circuits and Systems (MICS) Group Bradley Department of Electrical and Computer Engineering Virginia Tech, Blacksburg, Virginia, 24061, USA Email: {wjinhua6, ha}@vt.edu <sup>2</sup>Department of Advanced Railroad Vehicle Research Korea Railroad Research Institute (KRRI) Uiwang, 16105, Korea Email: lapin95@krri.re.kr

Abstract— The proposed powerline energy harvesting circuit aims to prevent saturation of a magnetic core, resulting increase of the harvested energy. The proposed magnetic field energy harvester (MFEH) has two secondary coils, the original one to harvest energy from the primary powerline and the additional one to desaturate the magnetic core. When the magnetic core is saturated by the magnetic field generated by the powerline, current starts to flow through the additional coil to desaturate the core. The desaturation controller is composed of a current sensor and a microcontroller unit (MCU) with associated switches. Experimental results show that the proposed circuit harvests 42.7 mW under powerline current of 25 A in rms. The circuit increases the amount of harvested power by 5.2 mW or 13.7 % through desaturation of the core.

Keywords— Powerline energy harvesting, current transformer, magnetic field energy harvester, magnetic core saturation.

#### I. INTRODUCTION

Nowadays, massive deployment of wireless IoT (Internet of Things) devices makes replacing or recharging of batteries expensive or impractical. Energy harvesting is a promising solution, and intensive research was performed to harvest power from various ambient resources including thermal, vibrational, solar, wind, RF sources, and powerlines [1]-[5]. AC powerlines are a stable energy source in urban and rural environments. Many researchers investigated methods to harvest energy from powerlines, often to power wireless IoT devices [6]-[9].

The performance of a magnetic field energy harvester (MFEH) for a powerline depends on several parameters including geometry, saturation, and nonlinearity of the core, position of the harvester, and the distance from the powerline [10]-[12]. Impact of the saturation and nonlinearity of magnetic cores is investigated in [13]. Design issues for power management circuits for powerline energy harvesting are impedance matching under powerline current and load variations, wake-up circuit, cold-start, and output voltage regulation. The duty cycle or the switching frequency of a DC-DC converter is often adjusted for impedance matching [5], [14]-[16], and maximum power point tracking (MPPT) aims to maintain impedance matching under varying operating conditions [1].

In this paper, we present a powerline energy harvesting circuit with a desaturation controller to reduce saturation of the magnetic core. In addition to the original secondary coil for the power stage, an additional secondary coil, called desaturation coil in this paper, is added to the MFEH. The direction of the powerline current sensed by a current sensor is applied to a microcontroller unit (MCU), which sets the direction of the desaturation coil current opposite to the direction of the powerline current. So, the magnitude of the

excessive magnetic field strength is decreased to reduce saturation of the magnetic core so that more energy can be harvested. The MCU and the controller for the desaturation are powered externally for the proposed circuit, but they can be powered by the harvested energy.

This paper is organized as follows. Section II reviews magnetic field energy harvesters, magnetic core saturation, existing desaturation techniques and negative voltage converter. Section III presents the proposed circuit and explains its operation. Section IV presents an experiment setup and measurement results. Section V concludes the paper.

#### II. PRELIMINARIES

#### A. Magnetic Field Energy Harvester (MFEH)

An MFEH shown in Fig. 1 is composed of a winding coil around a ferrite core. In essence, it is a current transformer and commonly used for powerline energy harvesting [5]. The number of turns of the coil and the geometry of the ferrite core determine the performance of the MFEH to harvest electromagnetic power as investigated in [10].

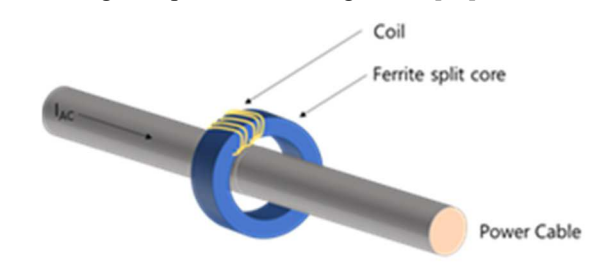


Fig. 1. Magnetic field energy harvester.

Fig. 2 shows an equivalent circuit model of a typical MFEH. The number of turns on the primary side is 1 and so represented as a wire.  $L_{Eff}$  is the effective inductance,  $L_{Leak}$  the leakage inductance, and  $R_{Wire}$  the wire resistance of the coil. When the magnetic core is saturated,  $L_{Eff}$  drops significantly, which causes a large amount of current to flow through  $L_{Eff}$ , resulting small current through the load or a small amount of energy harvested.

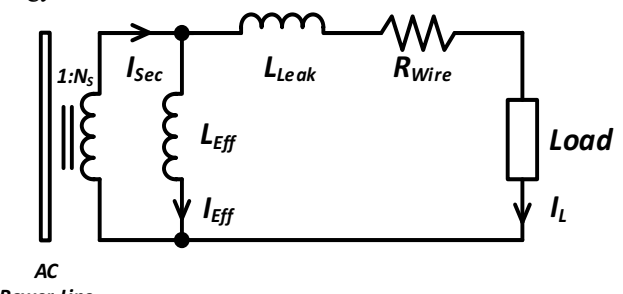


Fig. 2. Equivalent circuit of an MFEH.

#### B. Magnetic Core Saturation

Fig. 3 shows a typical B-H curve of a magnetic core. As the magnitude of the magnetic field strength  $\vec{H}$  increases, the magnitude of the magnetic flux density  $\vec{B}$  increases linearly initially, but it becomes saturated due to saturation of the magnetic core. The induced current  $\vec{I_S}$  on the secondary side is as follows.

$$\overrightarrow{I_S} \propto \left| \frac{d\overrightarrow{\phi}}{dt} \right| = S \left| \frac{d\overrightarrow{B}}{dt} \right|$$
 (1)

where  $\overline{\Phi}$  is magnetic flux, and S is the area of the cross-section through which the magnetic flux passes. When the magnetic core is saturated,  $\frac{d\overline{B}}{dt} \approx 0$  and hence  $\overline{I_S} \approx 0$ , resulting little energy being harvested. The B-H curve is determined by the material properties of the magnetic core.

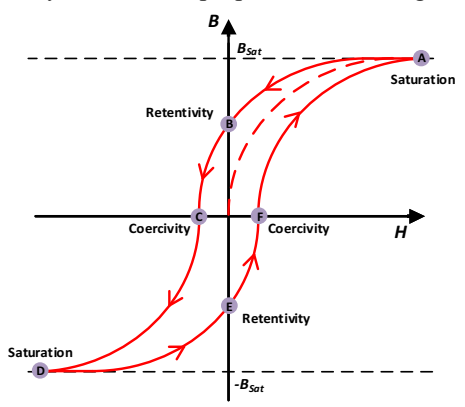


Fig. 3. Typical B-H curve of a magnetic core.

The B-H relationship is linearized and expressed as an arctangent function as show in (2) [17].

$$B(t) = B_{Sat} \frac{2}{\pi} \tan^{-1}(\beta H(t))$$
 (2)

where  $\beta$  is a constant representing sensitivity of the core in the linear region and determined by the material property of the magnetic core. A linearized B-H curve is shown in Fig. 4. It is divided into three regions, one linear region and two saturation regions. The proposed method is to monitor if  $\vec{B}$  enters the saturation region based on the linearized model. If it does, it activates the desaturation coil to reduce  $\vec{H}$ , resulting  $\vec{B}$  moving back to the linear region.

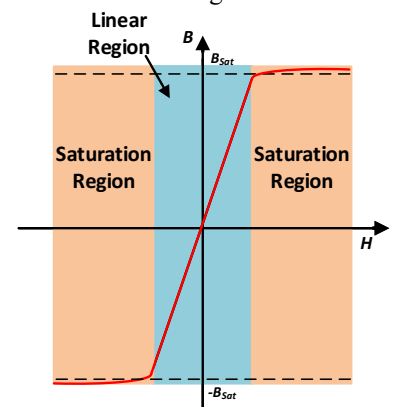


Fig. 4. Linearized B-H curve of a magnetic core.

Fig. 5 shows typical waveforms of the powerline current  $\overline{I_P}$  and the induced current  $\overline{I_S}$ . The induced current  $\overline{I_S}$  follows derivative of  $\overline{I_P}$  initially. When  $\overline{I_P}$  reaches a certain value, the magnetic core becomes saturated, and hence  $\overline{I_S}$  drops sharply

and reaches near zero eventually. The status of the magnetic core, saturated or not, can be identified roughly by sensing the induced current  $\overrightarrow{I_S}$ . The method is rather simple and adopted for the proposed circuit.

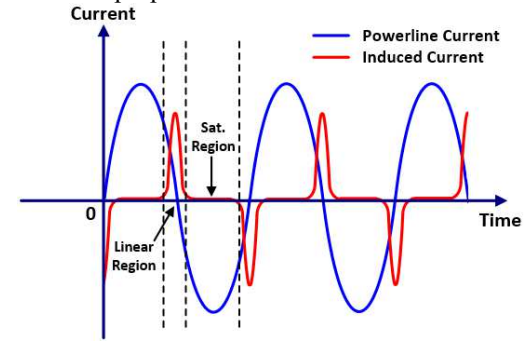


Fig. 5. Waveforms of powerline and induced currents.

#### C. Exsiting Desaturation Techniques

Paul et al. analyzed Si steel, Ni steel, and nano crystalline for the material of the MFEH core and proposed an MFEH with dual core [6]. Two cores made of different materials are integrated together. The inner core is made of Si steel due to its high  $B_{Sat}$ , and hence the core remains in the linear region mostly. The outer core is made of Ni steel due to its high permeability and low core loss. However, this design does not address the fundamental problem of core saturation , as large powerline current can reach the saturation region.

Zhuang et al. proposed a powerline energy harvesting system with a desaturation coil for the magnetic core [7]. An additional secondary coil is winded to the magnetic coil, controlled by an MCU, and a battery powers the MCU. When the magnetic core is saturated due to the excessive strength of the magnetic field generated by the powerline current, a DC current in the opposite direction to the powerline current flows through the additional coil to reduce net magnetic field strength, and therefore achieve desaturation of the magnetic core. With the desaturation coil, the harvested power of the proposed circuit increases by a factor of 45%, and the circuit can harvest 283 mW, on average, under AC current of 10 A in rms at 50 Hz. One shortcoming of the circuit is that the activation time period of the desaturation controller is fixed. So, it is applicable only for a fixed power line current, and the line current usually varies.

#### D. Negative Voltage Converter

A negative voltage converter (NVC) shown in Fig. 6 is more efficient than a full-bridge rectifier, even with Schottky diodes, and hence adopted for the proposed circuit [3]. During the positive (negative) cycle of the input voltage, the PMOS  $M_1$  ( $M_2$ ) and NMOS  $M_4$  ( $M_3$ ) conduct, so that the current flows from node A (B) to the load. The diode  $D_1$  prevents the current from flowing in the reverse even if the load voltage is higher than the input voltage.

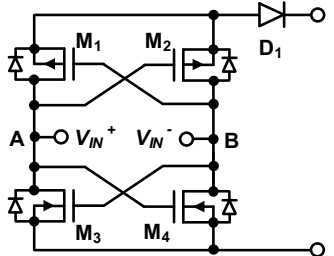


Fig. 6. Negative voltage converter.

#### III. PROPOSED CIRCUIT DESIGN

This section describes the proposed circuit, in which a desaturation controller is the core building block.

#### A. Block Diagram

Fig. 7 shows the block diagram of the proposed powerline energy harvesting circuit. The inductor  $L_1$  is the original secondary coil, and  $L_2$  is the additional secondary desaturation coil. A current sensor senses the induced current  $I_S$  and feeds the info to the MCU. When the magnitude of  $I_S$  reduces to the predetermined point, the magnetic core is saturated. The MCU turns on the relevant switches to flow  $I_D$  through  $L_2$ . The direction of  $I_D$  is set to the opposite to the direction of  $I_P$ . The magnetic core is desaturated to operate in the linear region. To demonstrate operation of the proposed circuit, the power for the desaturation controller and the current  $I_D$  is supplied externally. The power can be supplied from the harvested energy for real applications.

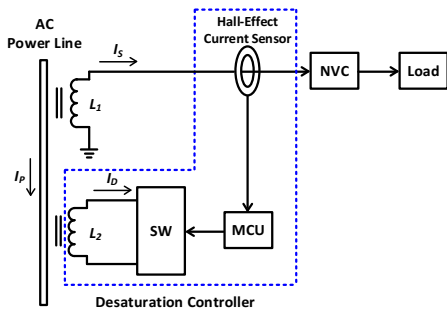


Fig. 7. Block diagram of the circuit.

### B. Circuit Diagram

Fig. 8 shows the schematic diagram of the proposed circuit. When the magnitude of the induced current  $I_S$  is greater than 0.5 mA, the core is considered as not saturated. The two switch signals  $S_1$  and  $S_2$  are low, which turn off all the transistors  $M_5 - M_8$ . The current  $I_D$  through  $L_2$  is zero. When the induced current is less than 0.5 mA, the core is saturated. The signal  $S_1$  ( $S_2$ ) becomes high if  $I_S$  is positive (negative).  $M_5$  and  $M_8$  ( $M_6$  and  $M_7$ ) are turned on to set  $I_D$  opposite of  $I_P$ . The net magnetic flux density  $\overline{B_{net}}$  is obtained as follows.

$$\overline{B_{net}} = \overline{|\overline{B_{L_1}}| - |\overline{B_{L_2}}|} \tag{3}$$

The resistors  $R_1$  and  $R_2$  are used to limit the magnitude of the desaturation current  $I_D$ .

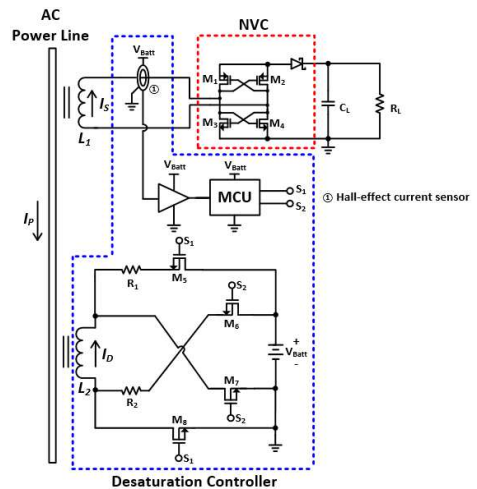


Fig. 8. Proposed powerline EH circuit with core desaturation.

#### IV. EXPERIMENTAL RESULTS

#### A. Prototype and Experiment Setup

Fig.9 shows a PCB prototype and experiment setup of the proposed circuit. The size of the PCB prototype is 51 mm by 110 mm. The MCU is Microchip Technology PIC16LF18446 on a development board DM164137, and the current sensor is TI TMCS1101. The powerline current is 25 A in rms with 50 Hz. The number of winding turns for both  $L_1$  and  $L_2$  is 100. Hereafter, all the current values are in rms unless stated otherwise.

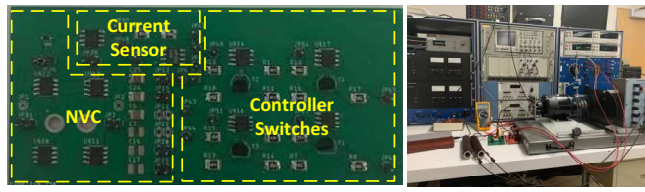


Fig. 9. (a) PCB prototype

(b) experiment setup.

#### B. Secondary Current in Different Regions

Fig. 10 shows the waveforms of the induced current  $I_S$  obtained under the powerline current  $I_P$  of 20 A and 25 A without the proposed desaturation controller. The load resistance  $R_L$  is set to 1 k $\Omega$  for both measurements. The waveform of  $I_S$  is sinusoidal with little distortion under  $I_P$ = 20 A, implying the magnetic core operates in the linear region. As  $I_P$  increases to 25 A, the core enters the saturation region for certain time periods. The induced current  $I_S$  drops sharply even though the powerline current increases. It results in reduction of the amount of power harvested.

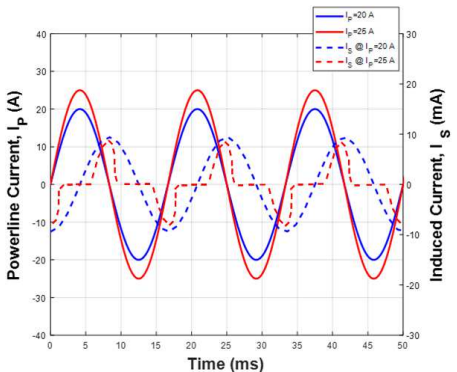


Fig. 10. Waveforms of the induced current  $I_S$  under the powerlne current of 20 A and 25 A.

Fig. 11 compares the waveforms of the induced current  $I_S$  with and without the desaturation controller with the load resistance  $R_L$  of 1.3 k $\Omega$  and 0.9 k $\Omega$ , respectively, under the powerline current  $I_P$  of 25 A. It is evident that the rms value of  $I_S$  increases with the desaturation controller, implying increase of the harvested power.

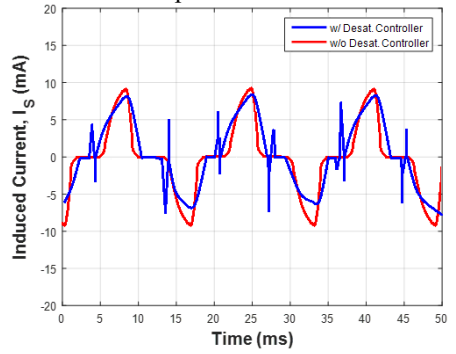


Fig. 11. Waveforms of the induced current  $I_S$  with and without the desaturation controller under the powerlne current of 25 A.

#### C. Harvested Power

The ultimate goal of the proposed desaturation controller is to increase the amount of power harvested. We measured the power delivered to the load resistor  $R_L$  for the proposed circuit with and without the desaturation controller. The current sensor is bypassed for "without" the desaturation controller and all the parts for the desaturation controller are disconnected. Fig. 12 shows the power delivered to the load or output power, in which  $R_L$  ranges from 0.1 k $\Omega$  to 3 k $\Omega$ . As R<sub>L</sub> increases the output power increases initially for both with and without the controller. The power starts to decrease after it hits the peak power. The peak power without the desaturation controller is 37.5 mW for  $R_L = 0.9 \text{ k}\Omega$ . The peak output power with the desaturation controller is 65.8 mW for  $R_L = 1.2 \text{ k}\Omega$ . The desaturation controller increases the peak power by 75.5%. Note that the optimal load resistance  $R_L$  for peak power is 1.2 k $\Omega$  with the desaturation controller and reduced to  $0.9 \text{ k}\Omega$  without the controller. It implies saturation of the magnetic core reduces the effective source impedance of the magnetic field energy harvester.

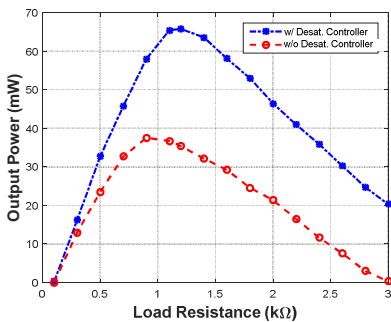


Fig. 12. Output power vs. load resistance with/without the desaturation controller

The desaturation controller dissipates power, which is a loss. Hence, the amount of the harvested power is reduced by the amount of power dissipated by the controller. Table I lists a breakdown of the power dissipation of the controller at the peak output power.

TABLE I POWER DISSIPATION BREAKDOWN

TOWER BROWN THIS CONTRACTOR	
Parts	Power Dissipation (mW)
Current Sensor TI TMCS1101	2.81
Microcontroller PIC16LF18446	0.54
Two MOSFET switches	1.59
One current-limiting resistor	18.2
TOTAL	23.14

The desaturation controller dissipates 23.14 mW in total. Therefore, the peak harvested power with the controller is 42.66 mW (= 65.8 mW - 23.14 mW), implying the proposed circuit increases the amount of harvested power by 13.8 %.

## V. CONCLUSON

A powerline energy harvesting circuit with a desaturation controller is presented in this paper. The proposed circuit adopts an MFEH with a desaturation coil to compensate the saturation effect of the magnetic core. The proposed circuit increases the harvested power by 5.2 mW or 13.8% compared

with a circuit *without* the controller under the powerline current of 25 A. For the proposed circuit, the current  $I_D$  for desaturation is fixed, resulting its effectiveness is limited for a certain range of the primary current. A powerline energy harvesting circuit with an adaptive desaturation controller is left for future work.

#### REFERENCES

- J. Wang, J. Li and D. S. Ha, "Energy Harvesting Circuit for Indoor Light Based on the FOCV and P&O Schemes with an Adaptive Fraction Approach," 2020 IEEE International Symposium on Circuits and Systems (ISCAS), Oct. 2020.
- [2] A. Jushi, A. Pegatoquet, and T. N. Le, "Wind Energy Harvesting for Autonomous Wireless Sensor Networks," Euromicro Conference on Digital System Design (DSD), Sept. 2016.
- [3] J. H. Hyun, L. Huang, and D. S. Ha, "Vibration and Thermal Energy Harvesting System for Automobiles with Impedance Matching and Wake-up," International Symposium on Circuits and Systems (ISCAS), May 2018.
- [4] R. Reed, F. L. Pour and D. S. Ha, "An Efficient 2.4 GHz Differential Rectenna for Radio Frequency Energy Harvesting," International Midwest Symposium on Circuits and Systems (MWSCAS), Aug. 2020
- [5] J. Wang and D.S. Ha, "A Wide Input Power Line Energy Harvesting Circuit for Wireless Sensor Nodes," International Symposium on Circuits and Systems (ISCAS), May 2021.
- [6] S. Paul, S. Bashir and J. Chang, "Design of a Novel Electromagnetic Energy Harvester With Dual Core for Deicing Device of Transmission Lines," in IEEE Transactions on Magnetics, vol. 55, no. 2, pp. 1-4, Feb. 2019.
- [7] Y. Zhuang et al., "Improving Current Transformer-Based Energy Extraction From AC Power Lines by Manipulating Magnetic Field," *IEEE Trans. on Industrial Electronics*, vol. 67, no. 11, pp. 9471-9479, Nov. 2020.
- [8] P. Kamat, D. Sutar, and P. Pavan Prasad, "Efficient Energy Harvesting Using Current Transformer for Smart Grid Application," International Conference on Trends in Electronics and Informatics (ICOEI), Tirunelveli, Dec. 2018.
- [9] X. Zhao, T. Keutel, M. Baldauf and O. Kanoun, "Energy harvesting for overhead power line monitoring," International Multi-Conference on Systems, Signals & Devices, Chemnitz, Mar. 2012.
- [10] J. D. Boles, B. Ozpineci, L. M. Tolbert, T. A. Burress, C. W. Ayers, and J. A. Baxter, "Inductive power harvesting for a touchless transmission line inspection system," IEEE Power and Energy Society General Meeting (PESGM), July 2016.
- [11] A. Abasian, A. Tabesh, A. Z. Nezhad, and N. Rezaei-Hosseinabadi, "Design Optimization of an Energy Harvesting Platform for Self-Powered Wireless Devices in Monitoring of AC Power Lines," *IEEE Trans. on Power Electronics*, vol. 33, no. 12, pp. 10308-10316, 2018.
- [12] T. Hosseinimehr and A. Tabesh, "Magnetic Field Energy Harvesting from AC Lines for Powering Wireless Sensor Nodes in Smart Grids," *IEEE Trans. on Industrial Electronics*, vol. 63, no. 8, pp. 4947-4954, Aug. 2016.
- [13] S. Yuan, Y. Huang, J. Zhou, Q. Xu, C. Song, and G. Yuan, "A High-Efficiency Helical Core for Magnetic Field Energy Harvesting," *IEEE Trans. on Power Electronics*, vol. 32, no. 7, pp. 5365-5376, 2017.
- [14] G. Yu, Z. Donglai, and H. Zhu, "Adaptive impedance matching optimal control method for cascaded DC-DC power supply system," in *IECON* 2017 - 43rd Annual Conference of the IEEE Industrial Electronics Society, Oct. 2017.
- [15] Y. Xu, D. S. Ha, and M. Xu, "Energy harvesting circuit with input matching in boundary conduction mode for electromagnetic generators," in 2017 IEEE International Symposium on Circuits and Systems (ISCAS), May 2017.
- [16] Y. Huang, N. Shinohara, and T. Mitani, "Theoretical analysis on DC-DC converter for impedance matching of a rectifying circuit in wireless power transfer," *IEEE International Symposium on Radio-Frequency Integration Technology (RFIT)*, Aug. 2015.
- [17] J. Moon and S. B. Leeb, "Analysis Model for Magnetic Energy Harvesters," IEEE *Trans.* on Power Electronics, vol. 30, no. 8, pp. 4302-4311, Aug. 2015.